

## Fragment angular distributions for neutron fission of $^{232}\text{Th}$

J. A. Becker and R. W. Bauer

*Lawrence Livermore National Laboratory, University of California, Livermore, California 94550*

(Received 5 September 1985)

Fission fragment angular distributions were measured for the neutron-induced fission of  $^{232}\text{Th}$  at incident energies from threshold to 6 MeV, using a white source of neutrons, time-of-flight techniques, and position-sensitive multiwire counters subtending a solid angle of nearly  $2\pi$  sr. The experimental data were analyzed in incident neutron energy bins of 40 keV and angular bins of 9 deg, and compared with previous results which were available for only partial energy ranges covered by this experiment. A channel analysis yielded relative strengths for the  $K$  transition states with  $K = \frac{1}{2}$ ,  $\frac{3}{2}$ , and  $\frac{5}{2}$  from threshold to  $E_n = 4.5$  MeV.

### I. INTRODUCTION

Resonance structures are observed in fast neutron-induced fission excitation functions of even-even actinide nuclei near threshold. For targets of  $^{230}\text{Th}$  and  $^{232}\text{Th}$ , the angular distributions of the fission fragments measured at these structures are found to change from peak to peak and within the 50–100 keV peak widths. The concept of the double-humped fission barrier provides the basis of an explanation for these structures.<sup>1</sup> The excitation energy relative to the ground state is  $\sim 6$  MeV; thus these peaks can be interpreted as manifestations of vibrational states (together with their rotational structure) in the second minimum of the potential surface. Studies of  $^{230}\text{Th}(n,f)$  at the isolated 720-keV resonance have been done with neutron energy resolution of a few keV. Analysis which requires a simultaneous good fit to both fission cross section and fragment angular distributions find good agreement with model predictions which employ a triple-humped barrier.<sup>2</sup> Furthermore, the well parameters are in accord with the predictions of Möller and Nix.<sup>3</sup> For the  $^{232}\text{Th} + n$  system, similar analyses have been made at incident neutron energies  $E_n = 1.6$  and 1.7 MeV.<sup>2,4,5</sup> Since these resonances are on a high background, interpretation in terms of a triple-humped barrier is less obvious.

The fragment angular distribution data are evidently crucial to the interpretation of the sub-barrier resonances. For example, the interpretation by Blons *et al.*<sup>2</sup> of the 720-keV  $^{230}\text{Th}$  resonance relies heavily upon the ratio of fission fragment yields measured by Veaser *et al.*<sup>6</sup> at angles  $\theta_f = 125^\circ$  and  $100^\circ$  with respect to the incident beam direction because of its statistical accuracy, and also upon the anisotropy measurements of Bruneau.<sup>7</sup> However, the fission fragment angular distribution data are presently not as complete as the cross-section data. The angular distribution data often cover a limited energy range, and they are not measured with energy resolution sufficient to distinguish the fine structure in the fission excitation function; this applies especially to those data obtained using a charged particle induced reaction as a source of neutrons. Data collected using a “white” neutron source produced at electron linac facilities most often represent the ratio of yields deduced from integral measurements made

with different angular ranges.

A method has been developed which measures the differential fission fragment yield with a large-area counter which subtends  $\sim 2\pi$  sr and which has good time resolution.<sup>8</sup> It is particularly useful for a “white” neutron source, where time-of-flight techniques are used to measure  $E_n$ , since a large solid angle device is important. Using this method, we have measured and report here the fragment angular distribution produced in the  $^{232}\text{Th}(n,f)$  reaction for the range of incident neutron energies  $0.72 \leq E_n(\text{MeV}) \leq 6.0$ . Limited by statistical accuracy, the data are presented in bins of  $\Delta E_n = 40$  keV.

Details of the experimental arrangement and data reduction are described in Sec. II. Since this is a new technique, extensive comparison with earlier results is also presented. For purposes of this comparison, the data are parametrized in a Legendre polynomial expansion. Section III presents analysis and discussion of the data in terms of the statistical theory of fission. Assuming a simplified reaction model, the distribution of  $K$  values of the compound nucleus at fission is presented as a function of  $E_n$  over the energy range  $0.72 \leq E_n(\text{MeV}) \leq 4.5$ . Section IV is a short summary.

### II. EXPERIMENT

#### A. Experimental arrangement

The experiment was carried out at the Lawrence Livermore National Laboratory 100-MeV Electron Linac Facility. A “white” neutron beam was obtained by irradiating a Ta target with a pulsed electron beam. The electron beam had the following characteristics: nominal energy  $E_e = 100$  MeV, average current 30  $\mu\text{A}$ , pulse width 3.5 nsec, and pulse interval 694  $\mu\text{sec}$ . The target consists of water cooled plates of Ta, nominally 50 mm thick. The energy distribution of neutrons is approximately Maxwellian with a characteristic energy of 1.6 MeV.

The 66 m time-of-flight station was used in this experiment. A combination of iron, polyethylene, boron, and carbon collimators was used to produce a beam spot of circular cross section (17.7 cm diam) at the sample. The size restriction of the beam spot was caused by the beam tube dimension rather than any inherent restriction in the

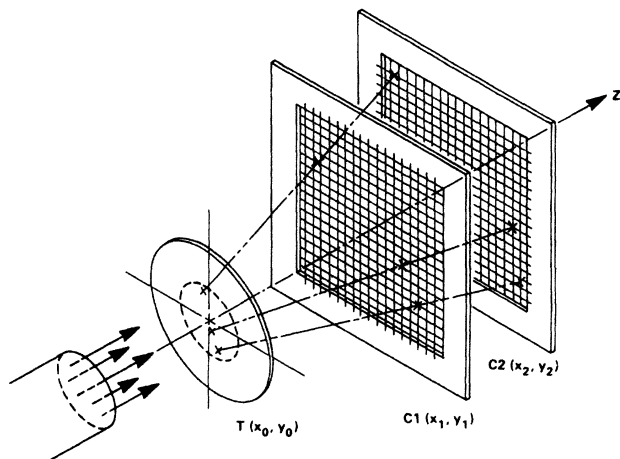


FIG. 1. Schematic experimental arrangement for the measurement of fission fragment trajectories. The chamber enclosing the counting gas, multiwire counters, and the fission foil is not shown.

counter. Neutron energy was determined using the time-of-flight technique, with a resolution of 92 psec/m.

Fission fragment angular distributions as a function of  $E_n$  were obtained using the following technique: A  $^{232}\text{Th}$  foil, 0.25 mm thick, was placed in front of two position-sensitive wire counters in a coplanar geometry. Foil and wire counters were enclosed in an Al box filled with a counting gas of  $\text{C}_4\text{H}_{10}$ , at a pressure 10 Torr. Beam entrance and exit windows were made of Al, 0.35 mm thick. The range for a 110 MeV fission fragment is approximately 275 cm in this environment. Thus, collecting data event by event, ray-tracing techniques can be used to determine the angle of the fragment relative to the incident beam direction,  $\theta$ , as the fragment leaves the Th sample. This arrangement is schematically illustrated in Fig. 1. Counters had active areas of  $25 \times 25 \text{ cm}^2$ . The intercounter distance was 40.1 mm, and the foil was 23.9 mm from the nearest counter. Each position-sensitive counter consisted of a central anode plane, together with two cathode planes. Interplane distance was 3.2 mm, and anode-cathode potential was +675 V. Anode wires were 20  $\mu\text{m}$  in diameter, and cathode wires were 100  $\mu\text{m}$  in diameter. The wire spacing for both anode and cathode planes was 2.54 mm. The cathode wires were connected to a tapped delay line; position readout is accomplished by time measurement of the charge centroid of the cathode pulse at one end of the delay line relative to the time of the anode pulse. The neutron energy for each event was deduced from the delay time of the anode pulse relative to the electron beam burst and the measured flight path distance.

These counters are operated in the avalanche mode; they are  $dE/dx$  devices, and fission fragments are distinguished from  $\alpha$  particles, e.g., by the different ionization in the active area of the counter, and the resulting different pulse heights. The counter parameters are arranged so that with a thin test source of  $^{252}\text{Cf}$  located on the counter axis, pulses induced by  $\alpha$  particles are in the

baseline noise, while pulses caused by fission fragments are concentrated in a band with a signal to noise ratio of  $\sim 10:1$ . The pulse height is approximately independent of angle; the angular resolution, full width at half maximum (FWHM), is  $3^\circ$  over an angular range  $\pm 65^\circ$ , and every fragment which passes through the counters produces a countable event, except for small edge effects.

During the experiment, acceptable events were required to have a minimum energy loss in both counters, set empirically in the following way: The  $^{232}\text{Th}$  foil was replaced by the  $^{235}\text{U}$  (93%) foil used for angular distribution normalization (see below). The pulse height distribution produced by the intense  $\alpha$  activity was observed, in turn, for all counter planes on the oscilloscope, and pulse height discrimination levels were set just above the maximum pulse height. When the samples ( $^{235}\text{U}$  or  $^{232}\text{Th}$ ) are irradiated with neutrons, only fragment events producing signals greater than this bias will be counted; thus only a selected sample of high energy fragments is taken from the continuum of fragments which emerge from the thick target with different mass, ionization state, and kinetic energy. The bias level is estimated at the energy loss of a 25 MeV fragment in one counter. With this bias, multiple scattering of fragments within the target does not distort the measured angular distribution (of those fragments counted) because the slowing down process for the fragments is dominated by electronic stopping. At 25 MeV, for example, the ratio of electronic to nuclear stopping is 60:1.

For the experiment, the chamber containing the fission foil and counters was rotated  $30^\circ$  about the vertical axis. The duration of the experiment was  $\sim 200$  h. More details are given in Ref. 8. A subset of the Fermi lab data acquisition code MULTI was used to collect data.<sup>9</sup>

## B. Data reduction

Data were sorted according to incident neutron energy  $E_n$  in 40 keV intervals and according to angle relative to the incident beam direction,  $\theta_f$ , in  $9^\circ$  intervals. The angular range was  $-72^\circ$  to  $99^\circ$ . (Angles labeled with the minus sign indicate a left handed rotation about the vertical axis.) The data were normalized to the angular distribution obtained for the  $^{235}\text{U}(n,f)$  reaction. These normalization data were obtained with the same experimental arrangement; however, the  $^{232}\text{Th}$  sample was replaced with a  $^{235}\text{U}$  foil (93% enrichment) 0.25 mm thick, and the incident neutron energy was required to be below 0.1 MeV. This results in an isotropic angular distribution of fragments. Thus, the ratio of counts obtained with the  $^{232}\text{Th}$  sample in place to that obtained with the  $^{235}\text{U}$  sample in place, for each angular bin, represents the angular distribution of the  $^{232}\text{Th}$  fragments corrected for geometrical effects, such as, for example, gradients in the detector plane distances or in the source-counter distance, or local variations in the counter efficiency.

The normalized angular distributions data were parameterized in terms of a Legendre polynomial expansion,

$$W(\theta) = I_f \left[ 1 + \sum_{k=2,4,6} A_k P_k(\cos\theta) \right]. \quad (1)$$

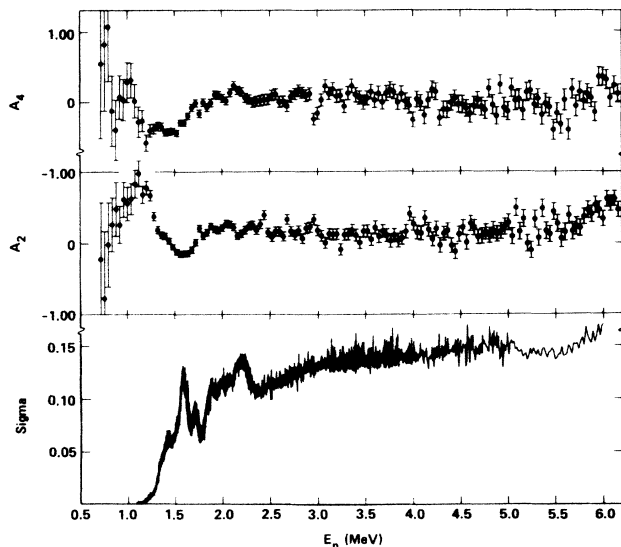


FIG. 2. Legendre polynomial coefficients characterizing the angular distribution of the fission fragments produced in the  $^{232}\text{Th}(n,f)$  reaction. The fission cross section (in barns) as measured by Blons *et al.* (Ref. 2) is given for reference.

The coefficients  $A_k$  obtained from a least-squares fit are presented as a function of  $E_n$  in Fig. 2, together with the cross section for the  $^{232}\text{Th}(n,f)$  reaction measured by Blons *et al.*<sup>2</sup> Figure 2 does not include  $A_6$  coefficients, since only at  $E_n = 1.40$  and  $1.60$  MeV was evidence found for a statistically significant  $A_6$  coefficient. For these energies, the results are given in Table I. A representative angular distribution obtained at  $E_n = 1.4$  MeV is presented in Fig. 3 to show the quality of the data and the Legendre polynomial fits.

### C. Characteristics of the data

The coefficients  $A_k$  exhibit broad structure below 2.0 MeV. There are also structures of width 50–100 keV throughout the data, e.g., the anomalies at  $E_n = 1.75$ , 2.98, and (possibly) 4.0 MeV. Distinct changes in  $A_k$  are not always correlated with structure in the  $(n,f)$  cross section, at, e.g.,  $E_n = 2.98$  MeV. Above 5.8 MeV the coefficient  $A_2$  begins an increase associated with the onset of

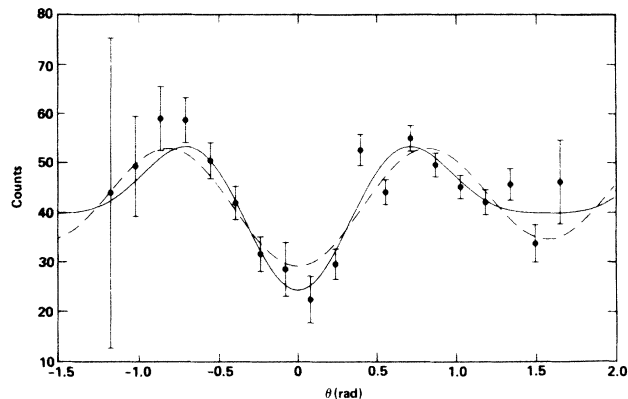


FIG. 3. Data points and Legendre polynomial fit of fission fragment angular distribution for  $^{232}\text{Th}(n,f)$  for  $1.40 \leq E_n(\text{MeV}) \leq 1.44$ . The dashed and solid curves represent the fits for  $k \leq 4$  and 6, respectively.

“second chance” fission. The  $A_k$  coefficients in the region  $2.2 < E_n(\text{MeV}) < 5.8$ , apart from the 50–100 keV wide fluctuations mentioned above, exhibit a smooth trend with increasing  $E_n$  up to  $E_n = 4$  MeV. Above this energy, further fluctuations may be present, but more data are required for a definitive statement.

### D. Comparison with previous data

Fragment angular distributions produced in the  $^{232}\text{Th}(n,f)$  reaction have been measured by Ermagambetov and Smirenkin,<sup>10</sup> Caruana, Boldeman, and Walsh,<sup>11</sup> and by Budtz-Jørgensen and Meadows.<sup>12</sup> Charged-particle neutron production reactions were used to obtain the neutron beams in these experiments. Collectively, these experiments include the incident neutron energy range from 0.9–2.3 MeV. Generally, the angular distributions are reported for a bin width  $\Delta E_n \sim 50$  keV; however, Budtz-Jørgensen and Meadows report distributions for very fine energy steps near 1.6 MeV. Intercomparison of these data shows general agreement for the trend of the Legendre polynomial expansion coefficients, although detailed examination shows disagreement (outside of statistical errors) at certain values of  $E_n$ . Illustrative examples are given in Table I.  $A_6$  coefficients in the results reported here are 0

TABLE I. Legendre polynomial expansion coefficients obtained from studies of the  $^{232}\text{Th}(n,f)$  fission fragment angular distribution.

Ref.	$E_n$ (MeV)	$\Delta E_n$ (MeV)	$A_2$	$A_4$	$A_6$
a	1.40	+0.04	+0.08(4)	-0.34(6)	-0.19(6)
a	1.60	+0.04	-0.17(4)	-0.21(5)	-0.16(5)
b	1.40	$\pm 0.02$	+0.00(2)	-0.10(3)	-0.15(3)
c	1.42	$\pm 0.05$	-0.04(2)	-0.21(2)	
a	Photo-fission <sup>d</sup>		-0.26(1)	-0.04(1)	

<sup>a</sup>This experiment.

<sup>b</sup>Reference 10.

<sup>c</sup>Reference 11.

<sup>d</sup>Refers to the fission products produced by  $^{232}\text{Th}(\gamma,f)$ .

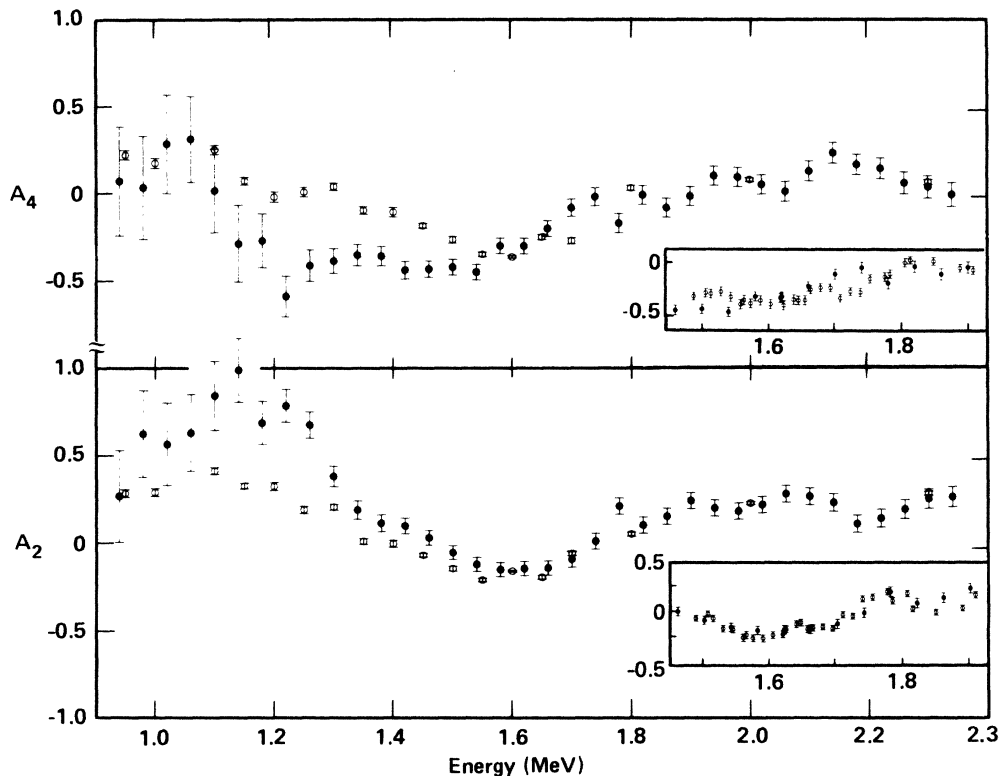


FIG. 4. The Legendre polynomial coefficients  $A_2$  and  $A_4$  derived from the fragment angular distribution of  $^{232}\text{Th}(n,f)$ , as a function of  $E_n$ . The present results (●) are compared with those of Ermagambetov and Smirenkin (Ref. 10) (○). The insets illustrate the results of Budtz-Jørgensen and Meadows (◻). The latter values, together with their errors, were deduced from graphical presentations in Ref. 12.

within two standard deviations, except as mentioned above (see Table I). Other authors have also reported nonzero  $A_6$  coefficients, particularly at  $E_n = 1.4$  MeV.

The angular distribution coefficients obtained in this experiment are compared with those reported by Ermagambetov and Smirenkin, and by Budtz-Jørgensen and Meadows in our Fig. 4. These data were selected because they span a wide range of incident neutron energies (0.95–2.30 MeV), Ref. 10, and include data obtained with neutron energy spread of  $\pm 8$  keV near  $E_n = 1.60$  MeV, Ref. 12. Agreement is good for the  $A_2$  coefficient except for the energy interval  $E_n = 1.1$ –1.3 MeV, where we find  $A_2$  coefficients larger than those of Ermagambetov and Smirenkin. There is general agreement for the  $A_4$  coefficients except for the interval 1.2–1.5 MeV, where the values reported here are more negative than those reported by Ermagambetov and Smirenkin. The inset of Fig. 4 compares the present results with those reported by Budtz-Jørgensen and Meadows. Good agreement for both  $A_2$  and  $A_4$  is obtained. It is difficult to understand why the coefficients  $A_2$  and  $A_4$  reported here differ so much with previous work at lower energies,<sup>10,11</sup> when both expansion coefficients agree well for  $E_n > 1.6$  MeV. The explanation probably does not lie in the use of a thick target or in the normalization technique. Ermagambetov and Smirenkin made a detailed study of the angular distribution of fission fragments obtained with both thick and thin targets (with appropriate normalization). They found

no significant difference in the fragment distributions over the incident neutron energy interval from 1.1 to 2.3 MeV. As a further check on our technique, we have analyzed the angular distribution of the photo-fission events, data with relatively good statistics. The angular distribution together with the results of the Legendre polynomial fit are presented in Fig. 5. The expansion coeffi-

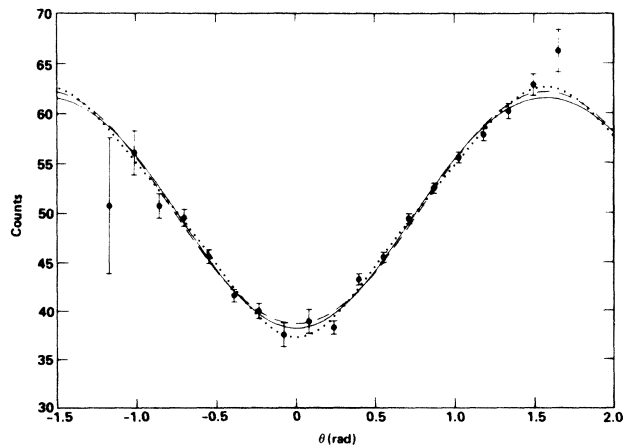


FIG. 5. Data points and Legendre polynomial description for the reaction  $^{232}\text{Th}(\gamma, f)$ . The dashed, solid and dotted curves represent the least-squares fits for  $k \leq 2$ , 4, and 6, respectively.

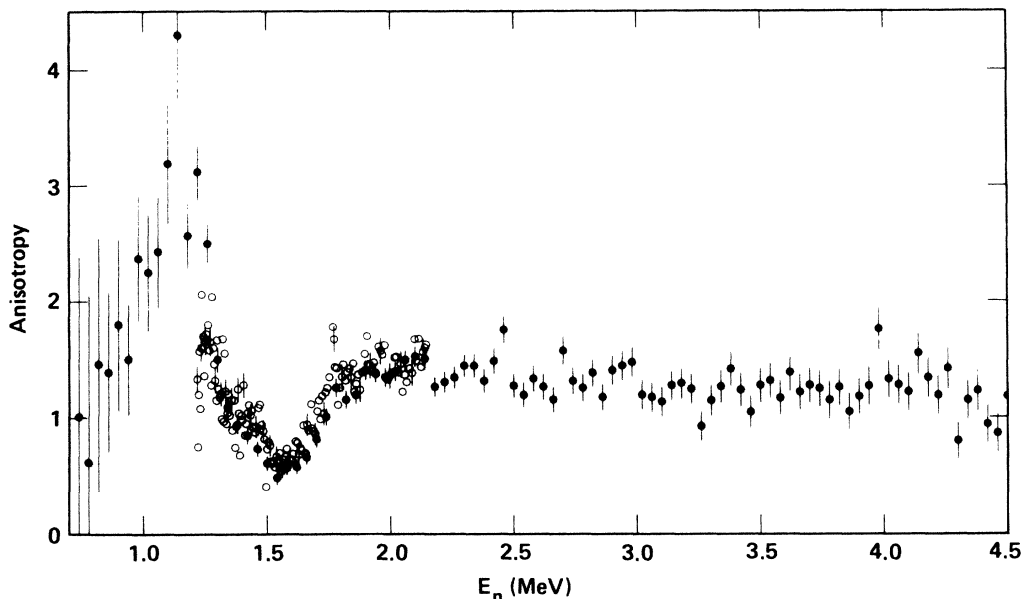


FIG. 6. Fission fragment anisotropy,  $W(0^\circ)/W(90^\circ)$ , vs  $E_n(\text{MeV})$  (●). For comparison, the anisotropy reported in Ref. 13 is presented (○).

coefficients are listed in Table I. The results are in accord with our expectation that  $A_2$  is large and  $A_4$  is small. There is no significant asymmetry about  $90^\circ$ , which would be indicative of instrumental misalignment or faulty procedure.

Figure 6 illustrates the anisotropy calculated from the present angular distributions, together with the anisotropy reported by Blons, Mazur, and Paya<sup>13</sup> over the range of incident neutron energy 1.2–2.1 MeV. Agreement is very good notwithstanding the  $A_K$  coefficient discrepancy noted above. Thus, full angular distribution measurements are necessary for detailed model evaluations, as also pointed out by Blons *et al.*<sup>2</sup>

### III. ANALYSIS AND DISCUSSION

We adopt the statistical model of fission, and present a simplified channel analysis of our data in this section. The distribution of  $K$  values in the fissioning nucleus may be obtained from the expression

$$W(\theta) = \sum_K A_K \sum_{J,\pi} B_{KJ}^\pi W_{KJ}(\theta), \quad (2)$$

where  $W_{KJ}(\theta)$  represents the expression for the angular distribution of fission fragments. The  $B_{KJ}^\pi$  represent the relative fission probability of the nucleus with quantum numbers  $J, K, \pi$ , and the coefficients  $A_K$  are the desired amplitudes, which we obtain from a least-squares fit of the data to Eq. (2).

The main assumptions are (1) the nucleus can be described by the eigenfunctions of the symmetric top,  $D_{MK}^J(\phi, \theta, \psi)$ , where  $\phi, \theta, \psi$  are the Euler angles and  $M, K$  are the projections of  $J$  onto the space-fixed axis and body-fixed axis, respectively, and (2) the fragments emerge along the nuclear symmetry axis. Specifically, for a spin  $\frac{1}{2}$  particle incident on an even-even target nucleus,  $W_{JK}(\theta)$  is given by

$$W_{KJ}(\theta) = \sum_J [(2J+1)/4] \times [ |d_{1/2,K}^J(\theta)|^2 + |d_{-1/2,K}^J(\theta)|^2 ], \quad (3)$$

where  $d_{MK}^J(\theta)$  represent the Jacobi polynomials. The distribution of  $K$  values of the transition state is determined assuming conservation of  $K$  from the transition state to fission. The quantities  $B_{KJ}^\pi$  are estimated as  $\sigma_f^\pi(J)/\sum \sigma_f^\pi(J)$ ; the partial fission cross sections are obtained from a Hauser-Feshbach calculation of the fission cross section for the reaction  $n + {}^{232}\text{Th}$  (Ref. 14). The calculation was done according to the prescription given by Bjørnholm and Lynn.<sup>1</sup> The quantities quoted by them in their Tables XXVIII, XXIX, and XXXI were used for estimates of the double-humped barrier heights and curvatures and for level densities. However, to describe the level density of  ${}^{232}\text{Th}$ , 20 measured levels were used below  $E_x = 1.121$  MeV rather than the Gilbert-Cameron form (expression 7.24 of Ref. 1). In this formulation neutron transmission coefficients were obtained from measured low energy  $s$ - and  $p$ -wave strength functions. The energy independent  $s$ - and  $p$ -wave strength functions were assumed for all even and odd values of  $l$ , respectively, as well as for inelastic channels. For the purpose of extracting the  $A_K$ , a smooth variation with incident neutron energy of the  $\sigma_f(J)$  together with a reasonable value of  $\sigma_f(J)/\sum \sigma_f(J)$  is more important than the absolute value of  $\sigma_f(J)$ . The results of the fit to Eq.(2), with  $\frac{1}{2} \leq K \leq \frac{5}{2}$ , and  $J \leq \frac{9}{2}$ , are shown in Fig. 7. The values shown represent the distribution of  $K$  values in the transition nucleus. Transmission resonances exhibiting a width of  $\sim 50$  keV are known in this region of incident neutron energy, and measured fragment angular distributions vary smoothly over these resonances.<sup>12</sup> Blons *et al.* (Ref. 2,

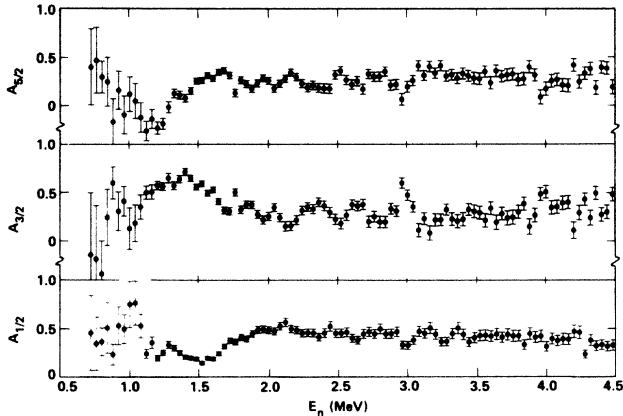


FIG. 7. Amplitudes  $A_K$  (in %) resulting from the channel analysis of the  $^{232}\text{Th}(n,f)$  fragment distribution as a function of incident neutron energy  $E_n$  (MeV).

Table VII) report relative  $K$  components integrated over 100-keV energy intervals. Similar quantities have been extracted from the work of Budtz-Jørgenson and Meadows, Ref. 12, Fig. 4. These amplitudes are compared with those found here in Table II.

There is rather rough agreement except at the 1.7 MeV anomaly, where Blons *et al.* report that  $K = \frac{3}{2}$  dominates while Budtz-Jørgenson and Meadows find that  $K = \frac{5}{2}$  dominates. However, we find the three amplitudes to be approximately equal. Our results (Fig. 7) also support the qualitative estimate of Blons *et al.* that the 1.05-MeV resonance has  $K = \frac{1}{2}$ . In the region of incident neutron energy between 1.1 and 1.3 MeV, the amplitude of  $A_{3/2}$  suggests that the contribution of  $K = \frac{3}{2}$  states to the cross section is more than previously recognized. Definitive statements for the other known transmission resonances below  $E_n = 1.3$  MeV cannot be made on the basis of these data because (i) the statistical quality of the data which is

TABLE II. Transition state amplitudes  $A_K$  (in %) deduced from channel analysis of angular distribution data.

$E_n$	Ref.	$A_{1/2}$	$A_{3/2}$	$A_{5/2}$
1.40	a	35	50	15
	b	23(2)	68(3)	9(3)
1.50	a	23	52	25
	b	16(2)	58(3)	26(3)
1.60	a	16	46	38
	b	19(2)	51(2)	29(2)
	c	14	45	41
1.71	a	32	49	19
	b	35(2)	31(3)	34(3)
	c	26	32	42

<sup>a</sup>Reference 2.  $\Delta E = 100$  keV.

<sup>b</sup>This work. Errors are statistical only.  $\Delta E = 80$  keV.

<sup>c</sup>Reference 12. Amplitudes are estimated from graphical data.  $\Delta E = 80$  keV.

TABLE III. Transition state amplitudes  $A_K$  (in %) deduced from channel analysis of angular distribution data. Errors are statistical only.  $\Delta E = 40$  keV.

$E_n$	$A_{1/2}$	$A_{3/2}$	$A_{5/2}$
0.92	38(15)	45(18)	0(22)
1.04	77(23)	18(19)	5(18)
1.16	36(6)	51(7)	-14(10)
1.20	20(3)	57(4)	-23(6)
1.28	33(4)	65(5)	2(6)

reflected in the wide neutron energy bin width is insufficient, and (ii) the negative values of  $A_{5/2}$  near  $E_n = 1.2$  MeV do not have physical meaning. The latter may be due to either incorrect experimental results in this region of  $E_n$  or an unduly simplified analysis. Table III summarizes the numerical values of  $A_K$  obtained at several known resonance energies.

Calculations have also been done for the structures at  $E_n = 1.4, 1.6,$  and  $1.7$  MeV, attempting a simultaneous fit to both the  $(n,f)$  cross section and the angular distribution/anisotropy data.<sup>2,4,5,11,15</sup> These calculations are done within the framework of the statistical model, and the concept of the double (triple)-humped fission barrier is integral to these calculations. The calculations produce a good fit to both cross section and angular distribution data; nevertheless, different conclusions about the relative  $A_K$  amplitudes are drawn. This is particularly evident at the 1.7 MeV resonance, where the analysis is expected to be more difficult and uncertain because of the background contribution from the states resonant at lower incident bombarding energies. For example, Boldeman<sup>15</sup> finds the 1.7 MeV resonance is  $K = \frac{5}{2}$ , while Auchampaugh *et al.*<sup>5</sup> find a mixture of  $K = \frac{1}{2}$  and  $\frac{3}{2}$  amplitudes, and Blons *et al.*<sup>2</sup> find the resonance is predominantly characterized by  $K = \frac{3}{2}$ .

At  $E_n \simeq 2.98$  MeV, there is a factor-of-2 fluctuation in  $A_{3/2}$  accompanied by decreases in  $A_{1/2}$  and  $A_{5/2}$ . There is no accompanying fluctuation in the fission cross section. The width of the fluctuation is consistent with the results of earlier work. This suggests that  $K$  is a good quantum number at this excitation,  $\sim 1.8$  MeV above threshold. The sudden increase in the density of levels with  $K = \frac{3}{2}$  may be a manifestation of the pairing interaction. Typically, the pairing energy gap parameter  $\Delta = 0.8$  MeV for light actinide nuclei at their equilibrium deformation. There is a preponderance of  $K = \frac{3}{2}$  states in the second well (at  $E_n = 1.35$  MeV), approximately 0.55 MeV below the fission barrier; thus it may not be unreasonable to find an increased level density for  $K = \frac{3}{2}$  states at an energy approximately  $2\Delta$  above the fission barrier.

#### IV. SUMMARY

New measurements of the fission fragment angular distributions for neutron-induced fission of  $^{232}\text{Th}$  have been carried out over a wide range of incident energies extend-

ing from threshold to the onset of second-chance fission, i.e., approximately  $0.72 \leq E_n(\text{MeV}) \leq 6.0$ . Angular distributions are reported for 40-keV increments of incident neutron energy. The white source of neutrons from an electron linac, time-of-flight techniques, and a multiwire detector system with high efficiency were utilized in this work. Our experimental results were compared with previous data sets, which, however, were available only over limited energy ranges. We found some discrepancies with existing data sets, especially in the lower energy range, but, in general, good agreement was achieved with the previously available data above  $E_n = 1.6$  MeV.

A statistical model channel analysis was made of these data, and as a result, the transition state amplitudes  $A_K$  ( $\frac{1}{2} \leq K \leq \frac{5}{2}$ ) were extracted over the neutron energy range  $0.72 \leq E_n(\text{MeV}) \leq 4.5$ . The reaction model details follow the prescription given in Bjørnholm and Lynn.<sup>1</sup> The  $A_K$  are in general agreement with earlier work where such measurements exist, within the energy step of the angular distributions reported here. At low incident neutron ener-

gies, the contribution from  $K = \frac{3}{2}$  states is more than has been generally accepted. A new anomaly in the angular distribution is observed at  $E_n = 2.98$  MeV, where there is no corresponding change in the fission cross section. Within the constraints of the analysis, this anomaly is interpreted as evidence that  $K$  remains a good quantum number  $\sim 1.8$  MeV above the fission threshold.

#### ACKNOWLEDGMENTS

We would like to express our appreciation to the Livermore Linac staff for continued assistance during the course of this experiment. We wish to thank J. Meadows for communication of unpublished results, and acknowledge discussions with J. Boldeman, J. Meadows, J. E. Lynn, R. White, and J. Trochon regarding this work. This work was performed under the auspices of the U.S. Department of Energy by the Lawrence Livermore National Laboratory under Contact No. W-7405-ENG-48.

<sup>1</sup>S. Bjørnholm and J. E. Lynn, *Rev. Mod. Phys.* **52**, 725 (1980).

<sup>2</sup>J. Blons, C. Mazur, D. Paya, M. Ribrag, and H. Weigmann, *Nucl. Phys.* **A414**, 1 (1984).

<sup>3</sup>P. Möller and J. R. Nix, in *Proceedings of the International Conference on the Physics and Chemistry of Fission, Rochester, 1973* (IAEA, Vienna, 1974), Vol. I, p. 103.

<sup>4</sup>H. Abou Yehia, J. Jary, J. Trochon, J. W. Boldeman, and A. R. de L. Musgrove, *Nuclear Cross Sections for Technology*, NBS Special Publ. No. 594 (U.S. Department of Commerce, Washington, D.C., 1980), p. 469.

<sup>5</sup>G. H. Auchampaugh, S. Plattard, N. W. Hill, G. deSaussure, R. B. Perez, and J. A. Harvey, *Phys. Rev. C* **24**, 503 (1981).

<sup>6</sup>L. R. Veaser and D. W. Muir, *Phys. Rev. C* **24**, 1540 (1981).

<sup>7</sup>B. Bruneau, Ph.D. thesis, Bordeaux University, 1980 (unpublished).

<sup>8</sup>J. A. Becker, *Nucl. Instrum. Methods* **211**, 297 (1983).

<sup>9</sup>J. F. Bartlett, J. R. Biel, D. B. Curtis, R. J. Dosen, T. R. Lagerlund, D. J. Ritchie, and L. M. Taff, *IEEE Trans. Nucl. Sci.* **NS-26**, 4427 (1979). The version of MULTI used here was due to T. Miles, University of British Columbia.

<sup>10</sup>S. B. Ermagambetov and G. N. Smirenkin, *Yad. Fiz.* **11**, 1164 (1970) [*Sov. J. Nucl. Phys.* **11**, 646 (1970)].

<sup>11</sup>J. Caruana, J. W. Boldeman, and R. L. Walsh, *Nucl. Phys.* **A285**, 205 (1977).

<sup>12</sup>C. Budtz-Jørgensen and J. Meadows, in *Proceedings of the International Symposium on Nuclear Fission and Related Collective Phenomena*, Bad Honnef, Germany (October, 1981), and private communication.

<sup>13</sup>J. Blons, C. Mazur, and D. Paya, *Phys. Rev. Lett.* **35**, 1749 (1975).

<sup>14</sup>R. M. White and R. E. Strout II, private communication.

<sup>15</sup>J. W. Boldeman, private communication.